



Contents lists available at ScienceDirect

Corrosion Science

journal homepage: www.elsevier.com/locate/corsci

Polyacrylic acid as a corrosion inhibitor for aluminium in weakly alkaline solutions. Part I: Weight loss, polarization, impedance EFM and EDX studies

Mohammed A. Amin^{a,c,*}, Sayed S. Abd El-Rehim^a, Essam E.F. El-Sherbini^a, Omar A. Hazzazi^b, Mohsen N. Abbas^d

^a Department of Chemistry, Faculty of Science, Ain Shams University, P.O. Box 11566, Abbassia, Cairo, Egypt

^b Department of Chemistry, Faculty of Applied Science, Umm Al-Qura University, P.O. Box 2897, Makkah, Saudi Arabia

^c Materials and Corrosion Lab (MCL), Department of Chemistry, Faculty of Science, Taif University, 888 Hawaiya, KSA

^d Paints and Chemical Industries (PACHIN)-Ameriya, Cairo, Egypt

ARTICLE INFO

Article history:

Received 22 October 2008

Accepted 8 December 2008

Available online xxxx

Keywords:

A. Aluminium

Weakly alkaline solutions

Corrosion inhibition

Polyacrylic acid

EFM

ABSTRACT

This part is devoted to study the influence of three selected polyacrylic acids (PAAs) with different molecular weights (PAA1 = 1800, PAA2 = 11,000 and PAA3 = 14,000 g mol⁻¹) on the corrosion inhibition of Al in weakly alkaline solutions (pH 8 and 10) at 30 °C. Measurements were conducted under different experimental conditions using chemical (weight loss) and electrochemical (potentiodynamic polarization and impedance) techniques, complemented with ex situ energy dispersive X-ray (EDX) examinations of the electrode surface. Electrochemical frequency modulation (EFM), a non-destructive corrosion measurement technique that can directly give values of corrosion current without prior knowledge of Tafel constants, is also presented here. The results demonstrated that these polymers inhibit the alkaline corrosion of Al. The inhibition effect of these polymers is due to their adsorption on Al surface. The isoelectric point (IEP) of aluminium oxide (pH 9) seems to be an important factor controlling corrosion inhibition and adsorption of the three polymers. The three polymers inhibit the corrosion reaction of aluminium excellently at pH 8, but less effectively at pH 10. Polarization measurements showed that the three polymers act as mixed-type inhibitors. The inhibition efficiencies of these polymers increase with increasing concentration, molecular weight and immersion time. Results obtained from the chemical and electrochemical measurements are in good agreements.

© 2008 Elsevier Ltd. All rights reserved.

1. Introduction

One of the most important applications of aluminium and its alloys is found in aluminium–air technology, firstly developed by Zaromb [1], which was of particular interest for its application to electric vehicle propulsion [2,3]. Amongst various types of anode materials, aluminium exhibits a high theoretical energy density (8.10 W h/g) combined with a high negative standard potential (–1.676 V vs. SHE) [4]. Further arguments for its consideration are its low production cost and the existence of a large base for manufacture and distribution.

Several attempts were made to develop a generator functioning in saline or acidic media [5–7], but in such conditions, the kinetics of aluminium dissolution are reduced by the presence of quite a thick oxide–hydroxide film at the anode surface [8]. This protective

film can only be broken by the presence of chloride ions in the solution [9,10], or by the action of strong alkaline solutions. Most of the workers have directed their research towards concentrated alkaline media, which permit optimal performances of the air cathode [11,12] as well as a low level of aluminium polarization during normal operation. However, aluminium suffers substantial corrosion in alkaline solutions, which induce coulombic loss on discharge and fuel loss during standby. Therefore, for commercial applications of the aluminium–air battery, it is necessary to add corrosion inhibitors, either to the metal or to the electrolyte, which are able to increase the overpotential of parasitic hydrogen evolution without decreasing the oxidation rate of aluminium.

Although sodium hydroxide exhibits a lower intrinsic conductivity than KOH, it is preferable because the aluminium oxidation product (NaAl(OH)₄) can be recycled through the Bayer process, a system available in the aluminium industry.

The relationship between structure dependent adsorption and corrosion inhibition is well known [13–16]. The corrosion inhibition of a metal involves strong adsorption of inhibitors to the metal surface by nitrogen, sulfur or oxygen and subsequent interference

* Corresponding author. Address: Department of Chemistry, Faculty of Science, Ain Shams University, P.O. Box 11566, Abbassia, Cairo, Egypt. Tel.: +20 222509331; fax: +20 24836831.

E-mail addresses: maaismail@yahoo.com (M.A. Amin), hazzazi@hotmail.com (O.A. Hazzazi).

with either cathodic or anodic reactions occurring at the adsorption sites. It is known that polymers are adsorbed stronger than their monomer analogs [16], hence it is expected that polymers will be better corrosion inhibitors than the corresponding monomers. The improved performances of the polymeric materials are ascribed to their multiple adsorption sites for bonding with the metal surface. The polymer provides two advantages: a single polymeric chain displaces many water molecules from the metal surface, thus making the process entropically favorable and the presence of multiple bonding sites make the desorption of the polymers a slower process.

Little seems to be published concerning the corrosion inhibition of Al using polymers [17,18]. For this reason, the objective of the present work is to investigate the corrosion inhibition of aluminium in weakly alkaline solutions, using three selected polyacrylic acids (supposed to be non-toxic [19,20]) with different molecular weights, under the influence of various experimental conditions including inhibitors concentration, solution pH, and immersion time. Weight loss, potentiodynamic polarization and EIS measurements were used in this study. As will be seen and fully discussed in the results and discussion part, polarization curves presented here show no linear Tafel region. The Tafel slopes are therefore impossible, and determination of j_{corr} (corrosion current density) from that impossible too. For this reason, electrochemical frequency modulation (EFM), a non-destructive corrosion measurement technique that can directly give values of corrosion current without prior knowledge of Tafel constants, is also presented here with the aim to make an accurate determination of the corrosion rate. Some EDX examinations of the electrode surface have been carried out.

2. Experimental

The working electrode employed in this work were made of spec pure aluminium (99.99% Koch Light Laboratories, Colnbrook Bucks, UK). The electrolytes investigated were 0.217 M sodium carbonate + 0.821 M sodium hydrogen carbonate (adjusted to the pH value 10 with aqueous NaOH solution). Bicarbonate buffer (pH 8.0) was prepared using 0.022 M sodium carbonate + 0.821 M sodium hydrogen carbonate [21]. For weight loss measurements, corrosion inhibition tests were performed using coupons measuring $1 \times 2 \times 0.1 \text{ cm}^3$ prepared from pure aluminium. The aluminium coupons were polished with emery papers, then degreased with acetone and washed with distilled water. The coupons were dried and kept in a desiccator. The weight loss (g cm^{-2}) was determined at different immersion times at 30 °C by weighing the cleaned samples before and after hanging the coupon into 50 cm^3 of the corrosive solution, namely the weakly alkaline solutions (pH 8 and 10), (in open air) in the absence and presence of various concentrations of the three selected polyacrylic acids. After the time elapsed (i.e., after an immersion time of 1.0 h) the cleaning procedure consisted of wiping the coupons with a paper tissue, washing with distilled water and acetone, followed by oven drying at 110 °C.

For electrochemical measurements, the investigated materials were cut as cylindrical rods, welded with Cu-wire for electrical connection and mounted into glass tubes of appropriate diameter using Araldite to offer an active flat disc shaped surface of (0.785 cm^2) geometric area, to contact the test solution. Prior to each experiment, the surface pretreatment of the working electrode was performed by mechanical polishing (using a polishing machine model POLIMENT I, BUEHLER POLISHER) of the electrode surface with successive grades of emery papers down to 1200 grit up to a mirror finish. The electrode was then, rinsed with acetone, distilled water, and finally dipped in the electrolytic cell.

A conventional electrochemical cell of capacity 100 cm^3 was used containing three compartments for working, platinum spiral

counter and reference electrodes. A Luggin–Haber capillary was also included in the design. The reference electrode was a normal calomel one used directly in contact with the working solution. The experiments were carried out in aerated stagnant buffer solutions (pH 8 and 10) devoid of and containing various concentrations of the three polymers. All solutions were prepared from analytical grade chemical reagents using doubly distilled water and were used without further purification. The potentiodynamic current–potential curves were recorded by changing the electrode potential automatically from -2.0 to 2.0 V at a scan rate of 0.10 mV s^{-1} .

EIS measurements were made using AC signals of amplitude 5 mV peak to peak at the open circuit potential (OCP) in the frequency range 100 kHz to 10 Hz. A Potentiostat/Galvanostat (EG&G model 273), lock-in amplifier (model 5210) and a personal computer were used. M352 corrosion software and M398 impedance software from EG&G Princeton Applied Research were used for the potentiodynamic polarization measurements and the EIS measurements, respectively.

EFM measurements were performed (using Gamry PCI300/4 Potentiostat/Galvanostat/Zra analyzer, DC105 Corrosion software, EIS300) with applying potential perturbation signal with amplitude of 10 mV with two sine waves of 2 and 5 Hz. The Intermodulation spectra contain current responses assigned for harmonical and intermodulation current peaks. The larger peaks were used to calculate the corrosion current density (I_{corr}), the Tafel constants (β_c and β_a) and the causality factors CF2 and CF3 [22,23].

EDX analysis was performed with Traktor TN-2000 energy dispersive spectrometer. Prior to analysis, the Al specimens were kept immersed in bicarbonate buffer solution (pH 8) for 12 and 24 h in the absence and presence of $2.0 \times 10^{-6} \text{ M}$ of the three polymers. Finally, the specimens were washed thoroughly and submitted to 5 min of ultrasonic cleaning in order to remove loosely adsorbed ions.

3. Results and discussion

3.1. Weight loss measurements

3.1.1. Effect of inhibitor concentration

The variation of the weight loss (g cm^{-2}) of Al in bicarbonate buffer solution (pH 8) with and without the addition of different concentrations (2.0×10^{-8} – $20.0 \times 10^{-8} \text{ M}$) of PAA1 with the immersion time has been studied at 30 °C; a part of the results is

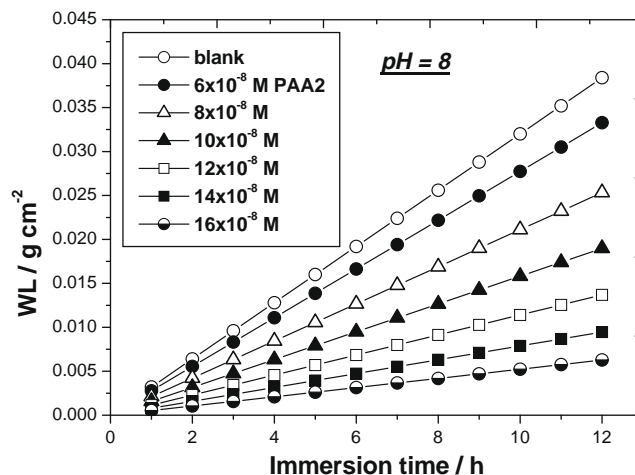


Fig. 1. Variation of the weight loss (in g cm^{-2}) of Al in bicarbonate buffer solution (pH 8) with and without the addition of different concentrations (6.0×10^{-8} – $16.0 \times 10^{-8} \text{ M}$) of PAA1 with the immersion time at 30 °C.

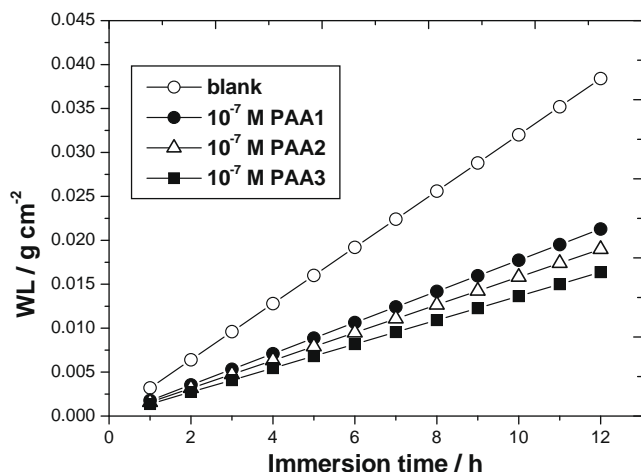
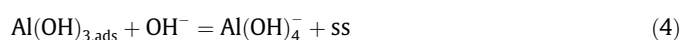
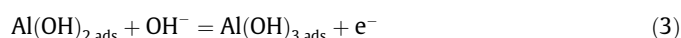
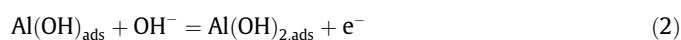


Fig. 2. Variation of the weight loss of Al in bicarbonate buffer solution (pH 8) containing the same concentration (1.0×10^{-7} M) of the three inhibitors with the immersion time at 30 °C.

shown in Fig. 1. Similar results were obtained for the other two polymers, namely PAA2 and PAA3. The weight loss of Al in bicarbonate buffer solution (pH 8) containing 1.0×10^{-7} M of the three polymers was determined as a function of the immersion time; the results are depicted in Fig. 2.

In aqueous alkaline media, Al reacts by the evolution of hydrogen. The evolution of hydrogen during this corrosion reaction may lead to serious pressure problems in industry. Detailed studies about these problems have been presented elsewhere [24,25]. Visual observations showed that the hydrogen evolution decreases (i.e., the corrosion-inhibiting effect increases) upon the addition of the three polymers. This could be seen from the weight loss decrease with increasing the concentration of each of these polymers (see Figs. 1 and 2). Thus, the corrosion rate of Al decreased with the increase of the polymer concentration. This trend may result from the fact that adsorption amount and the coverage of the polymer on the electrode surface increases with increasing concentration. Thus, the electrode surface is efficiently separated from the medium.

The corrosion process of Al in alkaline solution could be explained on the basis that the surface of Al is covered by passive film. When immersed in alkaline solutions, the outer surface of the film will dissolve, on the other hand, Al atoms in substrate will diffuse toward surface, or oxygen toward substrate, and combine to form passive film [26]. In some areas, the passive film is not very dense due to structural defects and is relatively more soluble, where its dissolution is faster than its formation. In these areas, dissolution of Al atoms and gradual removal of these atoms through the formation of hydroxide with increased coordination number from 1 to 3 to form independent molecular species of $\text{Al}(\text{OH})_3$ (see Eqs. (1)–(3)) takes place. $\text{Al}(\text{OH})_3$ species react in a pure chemical manner to form a soluble aluminate ion, $\text{Al}(\text{OH})_4^-$ that goes in solution leaving a bare surface site (ss) ready for another dissolution process (Eq. (4)) [27,28] Compared with the reduction of water, the reduction of oxygen can be neglected [26]. The corrosion process of Al in alkaline solution is usually considered as [28–30]:



As H_2 evolves (Eq. (6)), the local pH on bare surface site increases. This accelerates the corrosion reaction on them, and makes it easier for the passive film to be damaged.

The inhibition efficiencies (IE%) of the additives (Table 1) are calculated, after an immersion time of 1.0 h, from the total weight loss by the following equation:

$$\text{IE}\% = [1 - (\text{WL}/\text{WL}^0)] \times 100 \quad (7)$$

where WL^0 and WL are the weight losses of specimens without and with the inhibitor. It follows from the data of Table 1 that the three PAAs inhibit the alkaline corrosion of Al to an extent depending on their concentration and molecular weight. The IE% of the three polymers decrease in the order: PAA3 > PAA2 > PAA1. In all cases, increasing the additives' concentration is accompanied by an increase in the inhibition efficiency. It can also be seen from Table 1 that inhibition efficiency in all cases seems to reach a plateau value for high PAA concentrations. This trend can be explained as follows.

Since the primary action of inhibition is the adsorption of the PAA functional group onto the metal surface [31], adsorption is critical to corrosion inhibition. At high PAA concentrations (above 1.4×10^{-7} M), increasing inhibitor concentration leads to the gradual formation of multilayers that further reduce the rate of corrosion beyond what can be achieved with monolayer coverage below that concentration. However, results of the present work showed that concentration changes above 1.4×10^{-7} M of the three selected PAAs lead to minor changes in inhibition, inspect data presented in Tables 1 and 2 at $C_{\text{PAA}} > 1.4 \times 10^{-7}$ M, since the changes above that concentration result only in additional coverage beyond the monolayer level, which is already sufficient for significant inhibition. This situation is analogous to adding a second coating of paint to protect a surface that is already protected by an initial coating. In contrast, at PAA concentrations level well below 1.4×10^{-7} M, inhibition increases rapidly with increasing concentration, because the surface is filling with adsorbed PAA molecules from low coverage to monolayer coverage. Consequently, this critical concentration, namely 1.4×10^{-7} M may be a key indicator, under these experimental conditions, in determining the effectiveness of PAAs as corrosion inhibitors.

For further understanding we would say, transition from significant changes in inhibition efficiencies below 1.4×10^{-7} M to minor changes above that critical concentration may be indicative of the transition from traditional sub-monolayer-level adsorption to multilayer adsorption. It is possible that at a coverage of one monolayer or less, adsorbed PAA molecules can inhibit either the cathodic or anodic reaction by occupying reactive sites, or by simply providing resistance to the supply of oxidant or the transport of reaction products. Once the surface is filled with PAA molecules and additional molecules form multiple layer structures, the added PAA molecules no longer have direct access to the surface. Consequently, the additional molecules that adsorb at concentrations above 1.4×10^{-7} M may slightly inhibit corrosion by offering additional resistance (viscosity) to the transport of necessary elements rather than by occupying reactive sites directly.

3.1.2. Effect of solution pH

Fig. 3 illustrates the variation of the weight loss (g cm^{-2}) of Al in bicarbonate buffer solution (pH 10) with and without the addition of different concentrations (2.0×10^{-8} – 20.0×10^{-8} M) of PAA1 with the immersion at 30 °C. Similar results were obtained for PAA2 and PAA3. The inhibition efficiencies were determined at different concentrations of the three polymers at pH 10 and at 30 °C; the results obtained are listed in Table 2. The data presented in Ta-

Table 1
Values of IE% for Al in bicarbonate buffer solution (pH 8) containing various concentrations of the three inhibitors at 30 °C (weight loss, polarization, impedance and EFM measurements).

$(C \times 10^8)/M$	IE% (pH 8)									
	Weight loss			Polarization			Impedance			
	PAA1	PAA2	PAA3	PAA1	PAA2	PAA3	PAA1	PAA2	PAA3	
2.0	3.89	4.42	5.01	3.93	4.47	5.05	3.85	4.38	4.96	
4.0	6.08	6.90	7.83	6.14	6.98	7.89	6.012	6.83	7.75	
6.0	11.75	13.34	15.14	11.87	13.49	15.26	11.63	13.21	14.99	
8.0	29.99	34.04	38.63	30.29	34.41	38.94	29.69	33.70	38.24	
10.0	44.55	50.56	57.39	45.00	51.12	57.85	44.10	50.05	56.82	
12.0	56.70	64.35	73.04	57.27	65.06	73.62	56.13	63.71	72.31	
14.0	66.42	75.39	85.56	67.08	76.22	86.24	65.76	74.64	84.70	
16.0	73.71	83.66	94.96	74.45	84.58	95.72	72.97	82.82	94.01	
18.0	75.30	85.47	97.00	76.05	86.41	97.78	74.55	84.62	96.03	
20.0	76.00	86.26	97.91	76.76	87.21	98.69	75.24	85.40	96.93	
			IE% (pH 8) EFM							
			PAA1		PAA2		PAA3			
2.0			0.13		0.14		0.15		0.15	
4.0			0.15		0.16		0.17		0.17	
6.0			0.20		0.22		0.24		0.24	
8.0			0.36		0.40		0.43		0.43	
10.0			0.49		0.51		0.61		0.61	
12.0			0.60		0.66		0.74		0.74	
14.0			0.69		0.76		0.86		0.86	
16.0			0.76		0.84		0.95		0.95	
18.0			0.77		0.86		0.96		0.96	
20.0			0.78		0.87		0.98		0.98	

Table 2
Values of IE% for Al in bicarbonate buffer solution (pH 10) containing various concentrations of the three inhibitors at 30 °C (weight loss, polarization, impedance and EFM measurements).

$(C \times 10^8)/M$	IE% (pH 10)									
	Weight loss			Polarization			Impedance			
	PAA1	PAA2	PAA3	PAA1	PAA2	PAA3	PAA1	PAA2	PAA3	
2.0	2.33	2.76	3.23	2.36	2.79	3.29	2.29	2.71	3.19	
4.0	3.65	4.31	5.09	3.69	4.36	5.15	3.58	4.23	4.99	
6.0	7.05	8.34	9.84	7.13	8.43	9.95	6.91	8.17	9.64	
8.0	17.99	21.28	25.115	18.19	21.51	25.39	17.63	20.85	24.61	
10.0	26.73	31.60	37.30	27.02	31.95	37.71	26.20	30.97	36.56	
12.0	34.02	40.22	47.48	34.39	40.66	48.00	33.34	39.41	46.53	
14.0	39.85	47.12	55.61	40.29	47.64	56.23	39.05	46.18	54.50	
16.0	44.23	52.29	61.72	44.71	52.86	62.40	43.34	51.24	60.49	
18.0	45.18	53.42	63.05	45.68	54.00	63.74	44.28	52.35	61.79	
20.0	45.60	53.91	63.64	46.10	54.51	64.34	44.69	52.83	62.37	
			IE% (pH 10) EFM							
			PAA1		PAA2		PAA3			
2.0			2.45		2.91		3.42		3.42	
4.0			3.83		4.55		5.40		5.40	
6.0			7.40		8.80		10.43		10.43	
8.0			18.89		22.45		26.62		26.62	
10.0			28.07		33.34		39.54		39.54	
12.0			35.72		42.43		50.33		50.33	
14.0			41.84		49.71		58.95		58.95	
16.0			46.44		55.17		65.42		65.42	
18.0			47.44		56.36		66.83		66.83	
20.0			47.88		56.88		67.46		67.46	

bles 1 and 2 obviously show that, the inhibition efficiency values of the three polymers determined at pH 8 are greater than those obtained at pH 10. This means that the three polymers inhibit the aluminium corrosion more effectively at pH 8 than at pH 10.

These results could be explained with the isoelectric point (IEP) of aluminium oxide. It has been pointed out that in aqueous alkaline solutions, aluminium is always covered with aluminium oxide (or hydrated oxide) [21,32]. Since the IEP of aluminium oxide is at

about pH 9 [33], hence at pH 8 (below the IEP) the surface is positively charged, whereas it is negatively charged at pH 10 (above the IEP). Aliphatic carboxylic acids (e.g. PAA) have pK_a values <5 [33] and can be considered as dissociated to anions both at pH 8 and 10. So, at pH 8 (below the IEP) there should be an electrostatic attraction between the positively charged aluminium oxide surface and the negatively charged PAA (i.e., high IE%). On the other hand at pH 10 (above the IEP), both the aluminium oxide surface and the

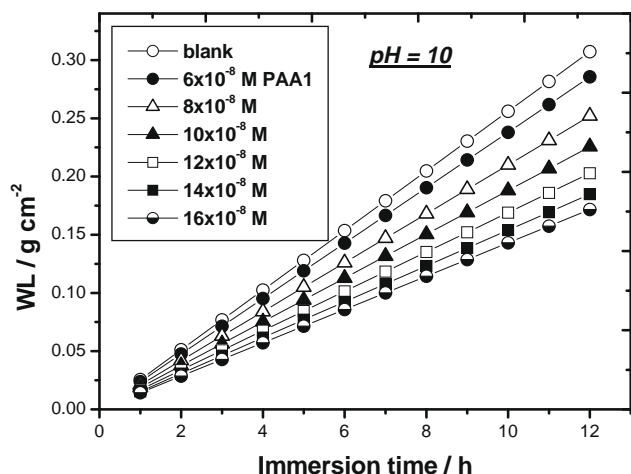


Fig. 3. Variation of the weight loss (in g cm^{-2}) of Al in bicarbonate buffer solution (pH 10) with and without the addition of different concentrations (6.0×10^{-8} – 16.0×10^{-8} M) of PAA1 with the immersion time at 30°C .

PAA are negatively charged, resulting in an electrostatic repulsion (i.e., low IE%).

It is well known that the improved performances of the polymeric materials as corrosion inhibitors are ascribed to their multiple adsorption sites for bonding with the metal surface [16]. These adsorption sites (negatively charged PAA) increase with increasing molecular weight of the polymer, and therefore, many water molecules will be displaced from the metal surface, thus making the process entropically favorable (i.e., high IE%), and this explains why the IE% increases with increasing molecular weight of the polymer following the sequence: PAA3 > PAA2 > PAA1.

3.2. Polarization measurements

3.2.1. Effect of inhibitor concentration

Fig. 4 shows the effect of PAA1 concentration on the potentiodynamic anodic and cathodic polarization characteristics of Al in bicarbonate buffer solution (pH 8) at a scan rate of 0.10 mV s^{-1} and at 30°C . Similar results were obtained for PAA2 and PAA3. The potentiodynamic anodic and cathodic polarization curves of

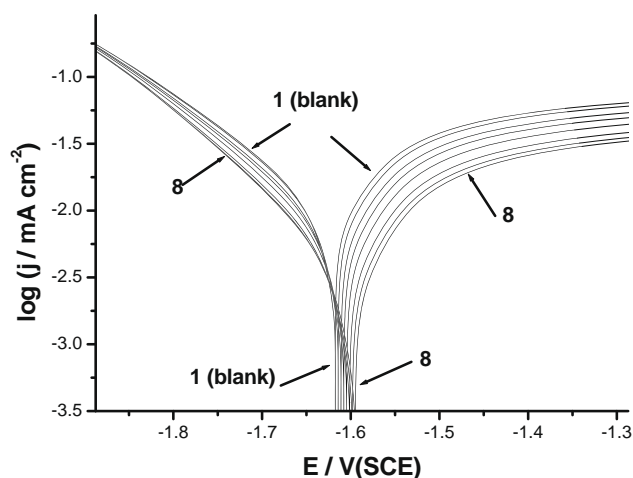


Fig. 4. Potentiodynamic anodic and cathodic polarization curves of Al in bicarbonate buffer solution (pH 8) in the absence and presence of various concentrations of PAA1 at a scan rate of 0.10 mV s^{-1} and at 30°C . (1) Blank; (2) 6.0×10^{-8} ; (3) 8.0×10^{-8} ; (4) 10.0×10^{-8} ; (5) 12.0×10^{-8} ; (6) 14.0×10^{-8} ; (7) 16.0×10^{-8} ; and (8) 20.0×10^{-8} M.

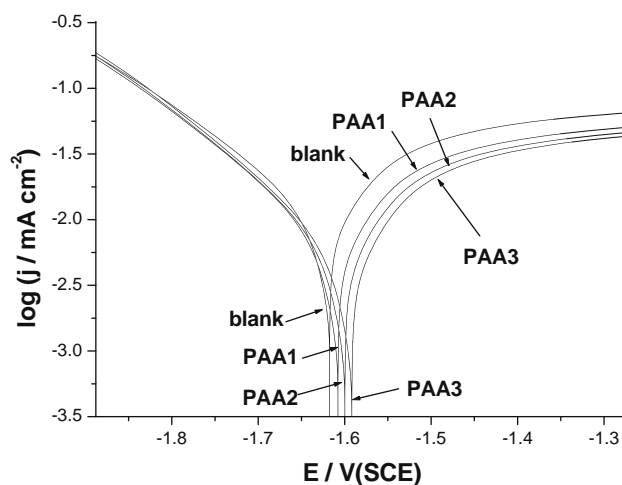


Fig. 5. Potentiodynamic anodic and cathodic polarization curves of Al in bicarbonate buffer solution (pH 8) containing the same concentration (1.0×10^{-7} M) of the three inhibitors at a scan rate of 0.10 mV s^{-1} and at 30°C .

Al in bicarbonate buffer solution (pH 8) containing 1.0×10^{-7} M of the three inhibitors at 30°C are presented in Fig. 5. The data clearly show that, the addition of the three polymers shifts the corrosion potential (E_{corr}) slightly in the positive direction and reduces both the anodic and cathodic current densities. The anodic current was, however, reduced, more significantly than the cathodic current. These results indicate that these polymers act as mixed-type inhibitors. This means that the three inhibitors have significant effects on retarding the cathodic hydrogen evolution reaction and inhibiting the anodic dissolution of aluminium.

The cathodic reaction which occurs when Al corrodes in weakly alkaline solutions has been investigated by Burstein and Liu [34]. Under the conditions used by Burstein and Liu, the cathodic reaction is primary the reduction of water to hydrogen according to the following reaction:



The overall anodic reaction in the corrosion of Al in weakly alkaline solutions is:



The electrochemical parameters (j_{corr} , E_{corr} , b_c and b_a and R_p) associated with polarization measurements of the three polymers at different concentrations were simultaneously determined and listed in Table 3.

According to the data of Table 3, it is obvious that the slopes of the anodic (b_a) and cathodic (b_c) Tafel lines remain almost constant upon the addition of each of these polymers. These results indicate that, these inhibitors act by simple blocking the available surface area for both anodic and cathodic processes. In other words, the inhibitors decrease the surface area for corrosion without affecting the mechanism of corrosion and only cause inactivation of a part of the surface with respect to the corrosive medium.

The inhibition efficiencies at different concentrations of the three inhibitors are calculated at pH 8 and 10 and listed in Tables 1 and 2, respectively, using the following equation:

$$P\% = 100 \times [(R_p - R_p^0)/R_p] \quad (10)$$

where R_p^0 and R_p are the electrode polarization resistances without and with inhibitor, respectively. Data of Tables 1 and 2 clearly show that in all cases, the inhibition efficiency increases with increasing additive concentration. Comparing the values of IE% of the three polymers at the same conditions (Tables 1 and 2), we find again that it decreases in the order: PAA3 > PAA2 > PAA1.

Table 3

The electrochemical parameters (j_{corr} , E_{corr} , b_c and b_a and R_p) associated with polarization measurements for Al in bicarbonate buffer solution (pH 8) in the absence and presence of different concentrations of the three inhibitors at 30 °C.

$(C \times 10^8)/M$	E_{corr}/V (SCE)			$(j_{\text{corr}} \times 10^3)/\text{mA cm}^{-2}$		
	PAA1	PAA2	PAA3	PAA1	PAA2	PAA3
0.0	-1.615	-1.615	-1.615	2.00	2.00	2.00
2.0	-1.614	-1.609	-1.604	1.92	1.91	1.90
4.0	-1.611	-1.605	-1.598	1.88	1.86	1.84
6.0	-1.608	-1.600	-1.592	1.77	1.73	1.70
8.0	-1.605	-1.595	-1.585	1.40	1.32	1.23
10.0	-1.601	-1.590	-1.579	1.11	0.99	0.85
12.0	-1.598	-1.585	-1.572	0.87	0.71	0.54
14.0	-1.595	-1.581	-1.566	0.67	0.49	0.29
16.0	-1.592	-1.575	-1.562	0.53	0.33	0.07
18.0	-1.590	-1.572	-1.560	0.49	0.29	0.06
20.0	-1.585	-1.570	-1.557	0.48	0.27	0.04

	$b_a/mV \text{ dec.}^{-1}$			$-b_c/mV \text{ dec.}^{-1}$			$R_p/\Omega \text{ cm}^2$		
	PAA1	PAA2	PAA3	PAA1	PAA2	PAA3	PAA1	PAA2	PAA3
0.0	51	51	51	26	26	26	300	300	300
2.0	50	49	52	25	24	25	312	314	316
4.0	49	50	49	24	25	24	319	322	325
6.0	50	51	50	25	24	24	340	346	354
8.0	51	48	49	24	23	23	429	455	489
10.0	52	49	51	24	26	24	541	607	704
12.0	48	51	49	23	27	25	693	842	1113
14.0	47	49	48	22	26	22	894	1219	2078
16.0	50	51	49	23	25	23	1141	1836	10399
18.0	51	49	49	24	25	24	1215	2064	10011
20.0	49	50	52	25	24	25	1250	2183	14320

Indeed, accurate evaluation of Tafel slopes by Tafel extrapolation is often impossible, simply because an experimental polarization curve does not exhibit linear Tafel regions [35–39]. Our experimental polarization curves presented here do not display the expected log/linear Tafel behaviour with both anodic and cathodic branches exhibiting curvature over the complete applied potential range. The curvature of the anodic branch may be attributed to the deposition of the corrosion products to form a non-passive surface film. With respect to the cathodic branch, since the solution is stationary, diffusion of oxidizing species (oxidants) will be slow, and concentration polarization can act to shorten the cathodic linear Tafel region. In the extreme case linearity may disappear altogether, with the cathodic reaction now under combined activation and diffusion control at E_{corr} .

As mentioned above, there is only one anodic (metal dissolution) and one cathodic (hydrogen evolution due to direct water reduction) reactions. As clearly seen from polarization curves, the cathodic branch exhibits no linearity or, what happens here to be a short Tafel region [35]. For these reasons, it was not possible to make an accurate evaluation of the anodic and cathodic Tafel slopes. If we do not have linear Tafel regions and Tafel slopes, we also cannot determine j_{corr} from polarization curves, even by extrapolation. If we extrapolated curved Tafel lines, we could read almost anything. Accordingly, we declare here that there is an uncertainty and source error in the numerical values of the Tafel slopes and j_{corr} , presented in Table 3, calculated by the software. On the same basis, we cannot determine j_{corr} from impedance plots, since these require Tafel slopes. For these reasons we used an alternative recent powerful method, namely electrochemical frequency modulation (EFM), to evaluate accurate values of the Tafel constants and j_{corr} ; see details in Section 3.4.

3.3. Impedance measurements

3.3.1. Effect of inhibitor concentration

Impedance measurements have been carried out for Al in the buffer solutions (pH 8 and 10) in the absence and presence of the

three polymers at the open circuit potential (OCP) under the influence of different experimental variables.

Fig. 6 illustrates the influence of PAA1 concentration on the impedance response of Al in bicarbonate buffer solution (pH 8) at OCP and at 30 °C. Similar results were obtained for PAA2 and PAA3. The Nyquist plots of Al in bicarbonate buffer solution (pH 8) containing the same concentration (1.05×10^{-7} M) of the three inhibitors at OCP and at 30 °C are presented in Fig. 7. The data reveal that, each impedance diagram consists of a large capacitive loop at high frequencies (HF), a small inductive one at medium frequencies (MF) followed by a second capacitive loop at low frequency values (LF). The HF capacitive loop could be assigned to the relaxation process in the aluminium oxide (or hydrated oxide) film presents on the aluminium surface and its dielectric properties [40,41]. Namely, the oxide film is considered to be a parallel circuit of a resistor due to the ionic conduction in the oxide film, and a capacitor due to its dielectric properties [41]. The electrode impedance in this case was determined by the metal/oxide interface, the oxide film, and the oxide/solution interface.

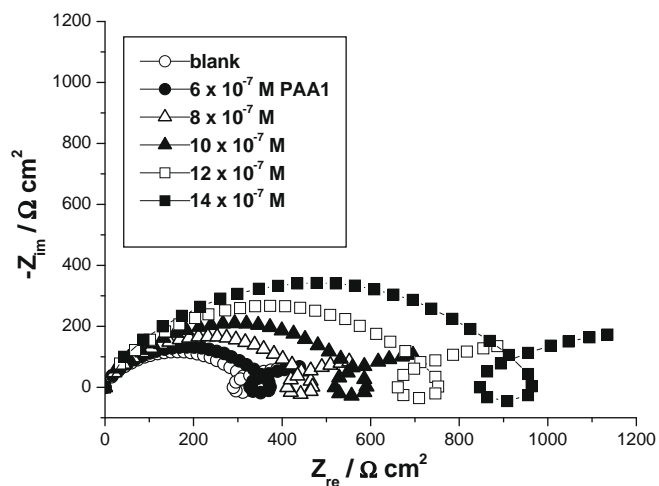


Fig. 6. Nyquist plots recorded for Al in bicarbonate buffer solution (pH 8) in the absence and presence of various concentrations of PAA1 at the OCP and at 30 °C.

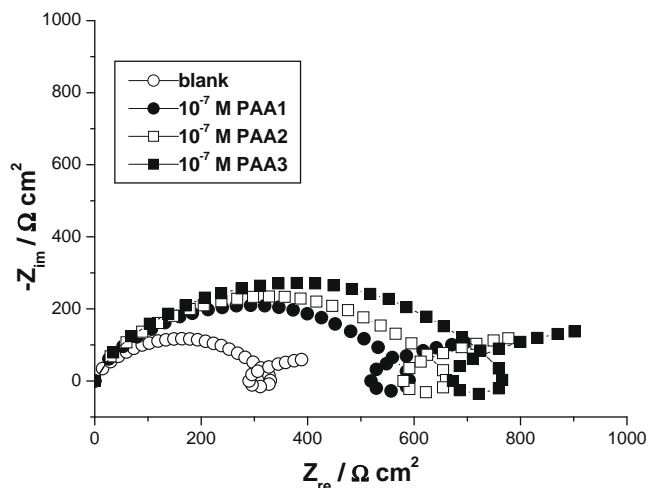


Fig. 7. The Nyquist plots of Al in bicarbonate buffer solution (pH 8) containing the same concentration (1.0×10^{-7} M) of the three inhibitors at OCP and at 30 °C.

Table 4

Numerical values of R_p and C_{dl} for Al in bicarbonate buffer solution (pH 8) in the absence and presence of various concentrations of the three inhibitors at OCP and at 30 °C.

$(C \times 10^8)/M$	$R_p/\Omega \text{ cm}^2$			$C_{dl}/\mu\text{F cm}^{-2}$		
	PAA1	PAA2	PAA3	PAA1	PAA2	PAA3
Blank	290.00	290.00	290.00	15.00	15.00	15.00
2.0	301.61	303.28	305.13	14.42	14.34	14.26
4.0	308.55	311.26	314.36	14.10	13.98	13.84
6.0	328.17	334.14	341.14	13.26	13.02	12.75
8.0	412.46	437.41	469.56	10.55	9.95	9.26
10.0	518.78	580.58	671.61	8.39	7.49	6.48
12.0	661.04	799.12	1047.31	6.58	5.44	4.15
14.0	846.96	1143.53	1895.43	5.14	3.80	2.30
16.0	1072.88	1688.01	4841.40	4.05	2.58	0.90
18.0	1139.49	1885.57	7304.79	3.82	2.31	0.60
20.0	1171.24	1986.30	9446.25	3.71	2.19	0.46

The HF capacitive loop makes an angle about 70° with the real axis and its intersection gives a value of (1.5 $\Omega \text{ cm}^2$) for the resistance of the solution (R_s) enclosed between the working electrode and the counter electrode (R_s). The inductive loop observed at MF may be attributed to the relaxation process in oxide presents on the electrode surface obtained by adsorbed species as OH_{ads} [26]. The point of intersection between the inductive loop and the real

axis represents ($R_s + R_p$), where R_p is the polarization resistance, which is defined as the dc limit of the impedance [42]. The second capacitive loop observed at LF values could be assigned to the metal dissolution. It is worthy noting that, the presence of these inhibitors does not alter the profile of the impedance spectra, suggesting similar mechanisms for the metal dissolution in the weakly alkaline solutions in the absence and presence of the inhibitor.

The numerical values of the polarization resistance (R_p) and the double layer capacitance (C_{dl}) were determined by analysis of the complex plane impedance plots and the equivalent circuit model by means of a computer program. Table 4 presents the values of R_p and C_{dl} recorded for Al in bicarbonate buffer solution (pH 8) in the absence and presence of various concentrations of the three inhibitors at OCP and at 30 °C.

It is obvious that in all cases, R_p values increase, while those of C_{dl} decrease with an increase in inhibitor concentration. The decrease in C_{dl} values is due to the adsorption of the inhibitor on the electrode surface [43]. It is found that the values of R_p decrease, while those of C_{dl} increase in the order: PAA3 > PAA2 > PAA1. These results confirm the results obtained from weight loss and polarization measurements that the inhibition efficiencies of the three polymers decrease in the same sequence.

The obtained R_p values were used to calculate the IE% of the three polymers at different concentrations (see Tables 1 and 2), using Eq. (10). It is apparent from the data of Tables 1 and 2 that the inhibition efficiencies of the three polymers obtained from chemical and electrochemical methods are in good agreements.

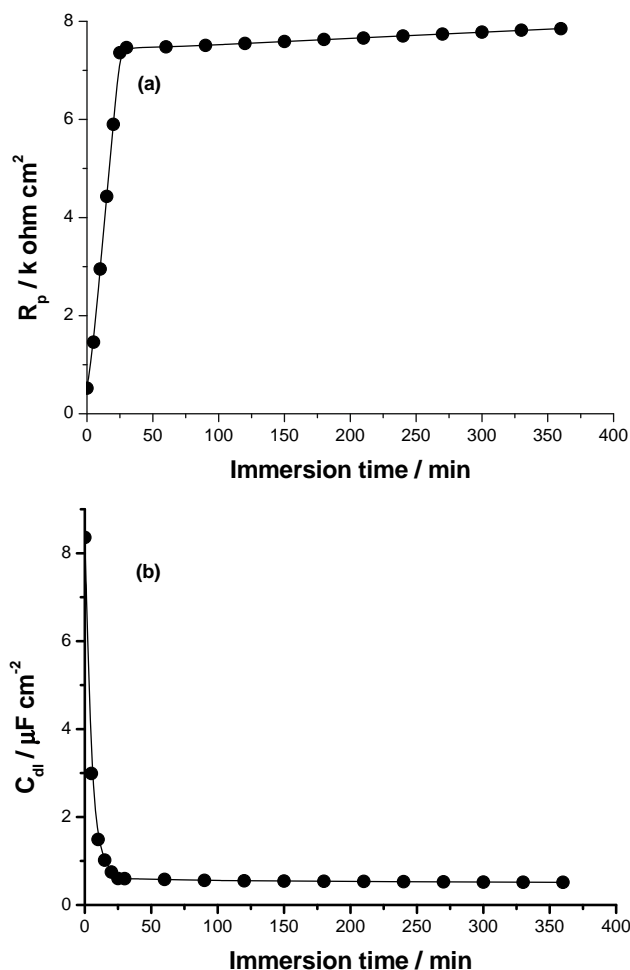


Fig. 8. The dependence of both R_p and C_{dl} on the immersion time for Al in bicarbonate buffer solution (pH 8) containing 1.0×10^{-7} M PAA1 at the OCP and at 30 °C.

3.3.2. Effect of the immersion time

Electrochemical impedance spectroscopy is a useful technique for long time tests, because they do not significantly disturb the system and it is possible to follow it overtime [44]. Immersion time experiments in the present work were carried out in bicarbonate buffer solution (pH 8) containing 1.0×10^{-7} M of the three polymers for 360 min and Nyquist plots were recorded every 5 min during the initial 30 min, and then every 30 min afterward. The re-

Table 5

The electrochemical kinetic parameters obtained by EFM technique recorded for Al in bicarbonate buffer solution (pH 8) in the absence and presence of different concentrations of the three inhibitors at 30 °C.

$(C \times 10^8)/M$	$(j_{\text{corr}} \times 10^3)/\text{mA cm}^{-2}$			$b_a/\text{mV dec.}^{-1}$		
	PAA1	PAA2	PAA3	PAA1	PAA2	PAA3
0.0	2.25	2.25	2.25	55	55	55
2.0	1.95	1.93	1.92	54	52	54
4.0	1.91	1.89	1.86	53	54	52
6.0	1.80	1.76	1.72	55	55	54
8.0	1.45	1.35	1.28	53	55	56
10.0	1.15	1.10	0.88	55	53	55
12.0	0.90	0.76	0.58	54	55	54
14.0	0.70	0.53	0.32	56	57	55
16.0	0.55	0.36	0.11	54	55	53
18.0	0.52	0.32	0.08	55	54	53
20.0	0.50	0.30	0.05	54	55	56

	$-b_c/\text{mV dec.}^{-1}$			Causality factor -2			Causality factor -3		
	PAA1	PAA2	PAA3	PAA1	PAA2	PAA3	PAA1	PAA2	PAA3
0.0	30	30	30	1.88	1.75	1.66	1.65	1.88	1.77
2.0	29	27	28	1.95	1.90	1.76	1.90	1.69	1.66
4.0	28	27	29	1.97	1.95	1.79	1.88	2.003	1.74
6.0	27	28	27	2.005	2.001	1.92	2.001	1.97	1.98
8.0	28	31	29	2.003	1.98	1.87	1.98	2.005	1.92
10.0	29	30	28	1.96	1.77	2.0005	1.88	1.94	1.91
12.0	30	29	29	1.89	1.73	2.007	1.80	1.83	1.79
14.0	28	29	27	1.85	1.81	1.86	1.75	1.79	1.88
16.0	30	29	28	1.90	1.75	1.96	2.0008	1.82	1.87
18.0	29	28	27	1.92	1.98	1.93	1.70	1.65	2.0007
20.0	31	27	28	1.95	1.88	1.96	1.88	1.97	2.008

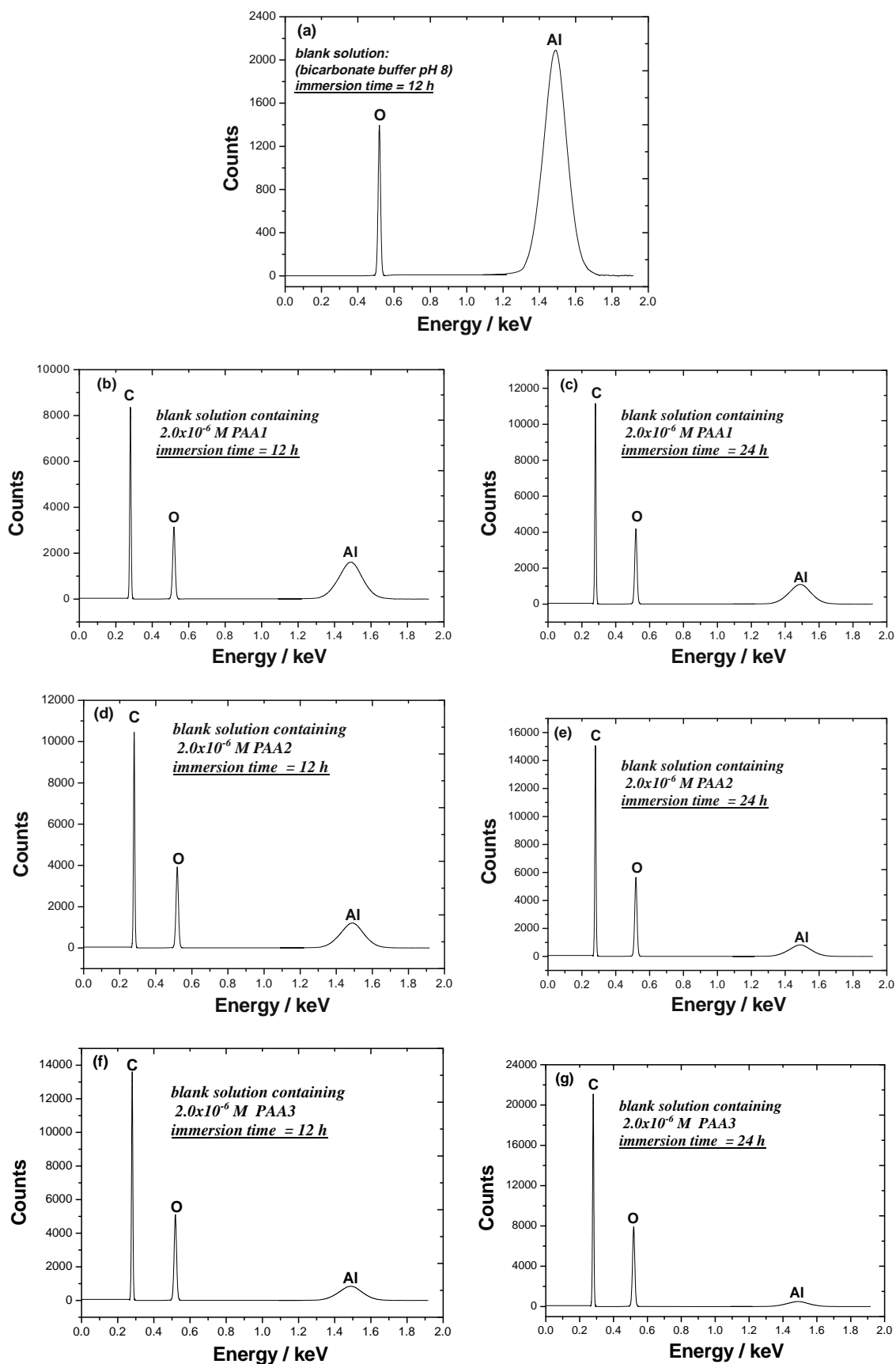


Fig. 9. EDX spectra recorded for Al specimens immersed in bicarbonate buffer solution (pH 8) for 12 and 24 h in the absence and presence of 2.0×10^{-6} M of the three polymers at 30 °C.

sults obtained (not shown here) showed that the immersion time has a great influence on the size and shape of the impedance spectra, and therefore the inhibition efficiency of the three polymers. The capacitive loop was found to increase in size with the increase of immersion time, reaching a maximum in 100 min and remained fairly constant afterward.

More details are shown in Fig. 8a and b, which represents the variation of both R_p and C_{dl} with the immersion time recorded for PAA1 (as a representative example); similar results were obtained for PAA2 and PAA3. It is obvious from Fig. 8a that the R_p values increased sharply from 0.52 to 7.35 $k\Omega\text{cm}^2$ during the initial 25 min and remained fairly constant afterward. At the same time, the capacitance values (Fig. 8b) were reduced drastically from 8.40 to 0.60 $\mu\text{F}/\text{cm}^2$ after 25 min and remained fairly constant afterward. This means that the formation of the inhibitor surface film, and therefore the inhibitor adsorption, on the electrode surface was fast and completed within 25 min.

These results demonstrate that the inhibition efficiency increases with increasing immersion time. This is consistent with the synergistic effect of polymer films (due to adsorption) and aluminium corrosion products to increase the protective power of the passive layer [25]. It is possible that with increasing immersion time and concentration, a compact adsorbed film of the inhibitor is formed on the aluminium surface, since more PAA anions electrostatically adsorb on the aluminium surface. The formation of such adsorbed film is confirmed by EDX examinations of the electrode surface (see Section 3.5). Competitive adsorption is assumed to occur on the aluminium surface between the aggressive OH^- ions and the anions of the inhibitor molecules [45].

If the corrosion process of Al is due to the adsorption of OH^- ions onto its bare metallic surface sites, as proposed by Macdonald [28], PAA anions will not compete with OH^- ions, but PAA adsorption can prevent OH^- ions to reach the Al sites by steric effect (may be one of the reasons why inhibition efficiencies of the three selected polymers increase in the order: PAA3 > PAA2 > PAA1 due to an increase in molecular weight). However, the mechanism proposed by Macdonald is not the only possible mechanism. Moon and Pyun [46] have proposed a mechanism where the $\text{Al}(\text{OH})_3$, see the chemical reaction in Eq. (3), are formed at the Al/oxide interface (no possible competition in this case), whereas Chu and Savinell [47] proposed a mechanism similar to that proposed by Macdonald, but involving Al^{3+} ions (competition possible).

3.4. Electrochemical frequency modulation measurements

The electrochemical frequency modulation (EFM) technique is a new tool for monitoring the electrochemical corrosion. The theory of EFM technique is previously reported [22]. Electrochemical Frequency Modulation technique has many features [22,23]:

- EFM is a non-destructive technique.
- EFM is a rapid test.
- EFM directly gives values of the corrosion current without a prior knowledge of Tafel constants.
- EFM has a great strength due to its the causality factors, which serve as an internal check on the validity of the EFM measurement.

The EFM intermodulation spectra (spectra of current response as a function of frequency) of Al in borate buffer solution (pH 8 and 10) devoid of and containing various concentrations of the three PAA's have been studied at 30 °C (data not presented here). The inhibition efficiencies were calculated at different PAA concentrations using equations presented elsewhere [48].

The calculated electrochemical parameters (j_{corr} , β_c , β_a , CF2, CF3 and IE%) are given in Table 5. Inspections of these data infer that

the values of causality factors obtained under different experimental conditions are approximately equal the theoretical values (2 and 3) indicating that the measured data are of quality [23]. Addition of increasing concentration of PAA to the buffer solution decreases the corrosion current density (I_{corr}) at a given temperature, indicating that PAA inhibits the corrosion of Al through adsorption. The calculated inhibition efficiency (IE%) enhances with PAA concentration. It is quite obvious that the data obtained from chemical and electrochemical measurements were in a good agreement with the results obtained from EFM.

3.5. EDX examinations of the electrode surface

EDX survey spectra were used to determine which elements were present on the Al surface before and after exposure to the inhibitor solution. After aluminium has been immersed in bicarbonate buffer solution (pH 8) in the absence and presence of 2.0×10^{-7} M of the three polymers for 12 and 24 h, its surface film composition was determined by EDX. The results are displayed in Fig. 9. For the electrode without inhibitor treatment (Fig. 9a), only aluminium and oxygen were detected, with a ratio of about 2:3, which indicated that the passive film contained only Al_2O_3 . However, in inhibited buffer solutions (Fig. 9b–g), the EDX spectra showed an additional line characteristic for the existence of C (due to the carbon atoms of the PAA). In addition, the O signal is significantly enhanced (due to the oxygen atoms present in the PAA). These data show that a carbonaceous material containing oxygen atoms has covered the electrode surface.

This layer is undoubtedly due to the inhibitor, because the carbon signal and the high contribution of the oxygen signal are not present on the electrode surface exposed to uninhibited buffer solutions (see Fig. 9a). In addition, the intensity of the carbon and oxygen signals increases with the immersion time (see Fig. 9b–g), since more PAA anions electrostatically adsorb on the aluminium surface. It is worth noting from the data presented in Fig. 9b–g that more PAA anions electrostatically adsorb on the Al surface for an immersion time of 24 h compared with 12 h, although the adsorption of the inhibitor on the electrode surface is completed within 25 min (monolayer coverage). This behaviour could be explained on the basis of the formation of multilayer of the adsorbed PAA anions on the electrode surface at long immersion times (see the possibility of transition from traditional submonolayer-level adsorption at low PAA concentrations and short immersion times to multilayer adsorption at high PAA concentrations and long immersion times fully discussed in Section 3.1.1).

It is obvious from the spectra of Fig. 9b–g that the Al peaks are dramatically suppressed relative to the samples prepared in the buffer solution, and this suppression increases with the immersion time. The suppression of the Al lines undoubtedly occurs because of the overlying inhibitor film. These results confirm the results obtained from polarization measurements that the inhibitor surface film retarded the cathodic hydrogen evolution reaction and inhibited the anodic dissolution of aluminium. It is possible that the inhibitor surface film acted as a barrier to the diffusion of H^+ ions from solution to electrode surface, which may increase the overpotential of the cathodic hydrogen evolution reaction, as shown in Fig. 4. This surface film also increased the polarization resistance of anodic dissolution of aluminium (see Fig. 6), slowing down the corrosion rate of aluminium in solution.

Fig. 9b, d and f clearly demonstrate that the contribution of the carbon and oxygen signals and the suppression of the Al lines increase in the order: PAA1 < PAA2 < PAA3. These results support the results obtained from chemical and electrochemical measurements that the inhibition efficiencies of the three polymers increase in the same sequence.

4. Conclusion

Chemical and electrochemical studies of the corrosion inhibition process of Al in weakly alkaline solutions using three selected polyacrylic acids as corrosion inhibitors showed that:

- (i) Addition of the three polymers to the alkaline solution inhibits the corrosion of Al. The inhibition is due to the adsorption of these compounds on the surface of Al.
- (ii) Polarization measurements showed that the three polymers function as a mixed-type inhibitor.
- (iii) Impedance measurements recorded for Al in the weakly alkaline solutions in the absence and presence of the three inhibitors showed that the Nyquist diagrams consisted of a large capacitive loop at high frequencies (HF), a small inductive one at medium frequencies (MF) followed by a second capacitive loop at low frequency values (LF).
- (iv) The inhibition efficiencies of these polymers increase with increasing their concentration, molecular weight and immersion time.
- (v) The inhibition efficiencies of the three inhibitors obtained from weight loss, potentiodynamic polarization and impedance methods are in good agreements with those obtained from the EFM technique.

References

- [1] S. Zaromb, The use and behavior of aluminum anodes in alkaline primary batteries, *J. Electrochem. Soc.* 109 (1962) 1125.
- [2] K.F. Blurton, A.F. Sammells, Metal/air batteries: Their status and potential – a review, *J. Power Sour.* 4 (1969) 263.
- [3] D.D. Macdonald, C. English, Development of anodes for aluminium/air batteries – solution phase inhibition of corrosion, *J. Appl. Electrochem.* 20 (1990) 405.
- [4] A.J. Bard, R. Parsons, J. Jordan, in: *Standard Potentials in Aqueous Solution*, Marcel Dekker, Inc., New York, 1985, p. 566.
- [5] A.R. Despic, D.M. Drazic, M.M. Purenovic, N. Coikovic, Electrochemical properties of aluminium alloys containing indium, gallium and thallium, *J. Appl. Electrochem.* 6 (1976) 527.
- [6] D.S. Keir, M.J. Pryor, P.R. Sperry, The influence of ternary alloying additions on the galvanic behavior of aluminum-tin alloys, *J. Electrochem. Soc.* 16 (1969) 319.
- [7] E. Budevski, I. Iliev, A. Kaisheva, A. Despic, K. Krsmanovic, Investigations of a large-capacity medium-power saline aluminium-air battery, *J. Appl. Electrochem.* 19 (1989) 323.
- [8] P.G. Anderson, O.F. Devereux, Steady-state anodic leakage current in barrier-type aluminium oxide films, *J. Electrochem. Soc.* 122 (1975) 267.
- [9] I.J. Albert, M. Kulandainathan, M. Anbu Ganesan, V. Kapali, Characterisation of different grades of commercially pure aluminium as prospective galvanic anodes in saline and alkaline battery electrolyte, *J. Appl. Electrochem.* 19 (1989) 547.
- [10] K. Nisancioglu, H. Holtan, Cathodic polarization of aluminium in acetate-buffered chloride media, *Electrochim. Acta* 24 (1979) 1229.
- [11] M. Rota, ch. Comminellis, S. Moller, F. Holzer, O. Haas, Bipolar Al/O₂ battery with planar electrodes in alkaline and acidic electrolytes, *J. Appl. Electrochem.* 25 (1995) 114.
- [12] V.P. Grigorev, V.V. Ekilic, Chemical Structure and Protective action of Corrosion Inhibitors, Restov University Edn, Ukraine, 1987.
- [13] A. Popova, M. Christov, S. Raicheva, E. Sokolova, Adsorption and inhibitive properties of benzimidazole derivatives in acid mild steel corrosion, *Corros. Sci.* 46 (2004) 1333.
- [14] A. Popova, M. Christov, A. Vasilev, Inhibitive properties of quaternary ammonium bromides of N-containing heterocycles on acid mild steel corrosion. Part I: Gravimetric and voltammetric results, *Corros. Sci.* 49 (2007) 3276.
- [15] S.N. Raicheva, B.V. Aleksiev, E. Sokolova, The effect of the chemical structure of some nitrogen- and sulphur-containing organic compounds on their corrosion inhibiting action, *Corros. Sci.* 34 (1993) 343.
- [16] *Encyclopaedia of Polymer Science and Technology*, second ed., Amorphous Polymers, Wiley, vol. 1, 1964, p. 558.
- [17] I.L. Lehr, S.B. Saidman, Characterisation and corrosion protection properties of polypyrrole electropolymerised onto aluminium in the presence of molybdate and nitrate, *Electrochim. Acta.* 51 (2006) 3249–3255.
- [18] I.L. Lehr, S.B. Saidman, "Electrodeposition of polypyrrole on aluminium in the presence of sodium bis(2-ethylhexyl) sulfosuccinate, *Mat. Chem. Phys.* 100 (2006) 262.
- [19] S. Majumdar, J. Dey, B. Adhahari, Taste sensing with polyacrylic acid grafted cellulose membrane, *Talanta* 69 (2006) 131–139.
- [20] S.-H. Huang, M.-H. Liao, D.-H. Chen, Fast and efficient recovery of lipase by polyacrylic acid-coated magnetic nano-adsorbent with high activity retention, *Sep. Purif. Technol.* 51 (2006) 113.
- [21] R.D. Armstrong, V.J. Braham, The mechanism of aluminium corrosion in alkaline solutions, *Corros. Sci.* 38 (1996) 1463.
- [22] R.W. Bosch, J. Hubrecht, W.F. Bogaerts, B.C. Syrett, Electrochemical frequency modulation: A new electrochemical technique for online corrosion monitoring, *Corrosion* 57 (2001) 60.
- [23] S.S. Abdel-Rehim, K.F. Khaled, N.S. Abd-Elshafi, Electrochemical frequency modulation as a new technique for monitoring corrosion inhibition of iron in acid media by new thiourea derivative, *Electrochim. Acta* 51 (2006) 3269.
- [24] B. Muller, Polymeric corrosion inhibitors for aluminium pigment, *React. Funct. Polym.* 39 (1999) 165.
- [25] B. Muller, M. Gampper, Corrosion and inhibition of corrosion of aluminium pigments in alkaline aqueous medium, *Werkst. Korros.* 45 (1994) 272.
- [26] W.J. Lorenz, F. Mansfeld, Determination of corrosion rates by electrochemical DC and AC methods, *Corros. Sci.* 21 (1981) 647.
- [27] F.M. Al-Kharafi, W.A. Badawy, Inhibition of corrosion of Al 6061, aluminum, and an aluminum-copper alloy in chloride-free aqueous media: Part 2 - Behavior in basic solutions, *Corrosion* 54 (1998) 377.
- [28] D.D. Macdonald, S. Real, S.I. Smedley, M. Urquidi-Macdonald, Evaluation of alloy anodes for aluminum-air batteries, *J. Electrochem. Soc.* 135 (1988) 2410.
- [29] D. Chu, R.F. Savinell, Experimental data on aluminum dissolution in KOH electrolytes, *Electrochim. Acta* 36 (1991) 1631.
- [30] M.L. Doche, J.J. Rameau, R. Durand, F. Novel-Cattin, Electrochemical behaviour of aluminium in concentrated NaOH solutions, *Corros. Sci.* 41 (1999) 805.
- [31] M.L. Free, Prediction and measurement of corrosion inhibition of mild steel using nonionic surfactants in chloride media, *Corros. Sci.* 46 (2004) 2601.
- [32] K. Aziz, A.M. Shams El Din, A simple method for the determination of the inhibition efficiency of surfactants, *Corros. Sci.* 5 (1965) 489.
- [33] R. Wood, D. Fornasiero, Electrochemistry of the boehmite – water interface, *Colloid Surf.* 51 (1990) 389.
- [34] G.T. Burstein, C. Liu, The cathodic reaction during repassivation of aluminium in open circuit, *Corros. Sci.* 37 (1995) 1151.
- [35] D.A. Jones, *Principles and Prevention of Corrosion*, Macmillan, New York, 1992, p. 96.
- [36] H.J. Flitt, D.P. Schweinsberg, A guide to polarisation curve interpretation: deconstruction of experimental curves typical of the Fe/H₂O/H⁺/O₂ corrosion system, *Corros. Sci.* 47 (2005) 2125.
- [37] J. Harvey, D. Flitt, Paul Schweinsberg, Evaluation of corrosion rate from polarisation curves not exhibiting a tafel region, *Corros. Sci.* 47 (2005) 3034–3052.
- [38] F. Mansfeld, Tafel slopes and corrosion rates obtained in the pre-Tafel region of polarization curves, *Corros. Sci.* 47 (2005) 3178.
- [39] B. Rosborg, J. Pan, C. Leygraf, Tafel slopes used in monitoring of copper corrosion in a bentonite/groundwater environment, *Corros. Sci.* 47 (2005) 3267.
- [40] F. Mansfeld, S. Lin, S. Kim, H. Shih, Pitting and surface modification of SiC/Al, *Corros. Sci.* 27 (1987) 997.
- [41] F. Mansfeld, S. Lin, S. Kim, H. Shih, Electrochemical impedance spectroscopy as a monitoring tool for passivation and localized Corrosion of aluminum alloys, *Werkst. Korros.* 39 (1988) 487.
- [42] H.J.W. Lenderink, M.V.D. Linden, J.H.W. De Wit, Corrosion of aluminium in acidic and neutral solutions, *Electrochim. Acta* 38 (1993) 1989.
- [43] F. Bentiss, M. Lagrence, M. Traisnel, J.C. Hornez, The corrosion inhibition of mild steel in acidic media by a new triazole derivative, *Corros. Sci.* 41 (1999) 789.
- [44] G. Moretti, F. Guidi, G. Grion, Tryptamine as a green iron corrosion inhibitor in 0.5 M deaerated sulphuric acid, *Corros. Sci.* 46 (2003) 387.
- [45] A.M. Beccaria, L. Chiaruttini, The inhibitive action of metacryloxypropylmethoxysilane (MAOS) on aluminium corrosion in NaCl solutions, *Corros. Sci.* 41 (1999) 885.
- [46] S.M. Moon, S.I. Pyun, The corrosion of pure aluminium during cathodic polarization in aqueous solutions, *Corros. Sci.* 39 (1997) 399.
- [47] D. Chu, R.F. Savinell, Experimental data on aluminum dissolution in KOH electrolytes, *Electrochim. Acta* 36 (1991) 1631.
- [48] S.S. Abdel Rehim, O.A. Hazzazi, M.A. Amin, K.F. Khaled, On the corrosion inhibition of low carbon steel in concentrated sulphuric acid solutions. Part I: Chemical and electrochemical (AC and DC) studies, *Corros. Sci.* 50 (2008) 2258.